Monthly Notices
of the
ROYAL ASTRONOMICAL SOCIETY

Mon. Not. R. Astron. Soc. (2010) doi:10.1111/j.1365-2966.2010.17027.x

The interplay of chaos between the terrestrial and giant planets

Wayne B. Hayes,[1,2]★ Anton V. Malykh[1] and Christopher M. Danforth[3]

[1]*Department of Computer Science, University of California Irvine, Irvine, CA, USA*
[2]*Department of Mathematics, Imperial College London, London SW7 2AZ*
[3]*Department of Mathematics and Statistics, Complex Systems Center, Vermont Advanced Computing Center, University of Vermont, Burlington, Vermont, USA*

Accepted 2010 May 14. Received 2010 April 14; in original form 2010 February 4

ABSTRACT

We report on some simple experiments on the nature of chaos in our planetary system. We make the following interesting observations. First, we look at the system of Sun + four Jovian planets as an isolated five-body system interacting only via Newtonian gravity. We find that if we measure the Lyapunov time of this system across thousands of initial conditions all within observational uncertainty, then the value of the Lyapunov time seems relatively smooth across some regions of initial condition space, while in other regions it fluctuates wildly on scales as small as we can reliably measure using numerical methods. This probably indicates a fractal structure of Lyapunov exponents measured across initial condition space. Then, we add the four inner terrestrial planets and several post-Newtonian corrections such as general relativity into the model. In this more realistic Sun + eight-planet system, we find that the above structure of chaos for the outer planets becomes uniformly chaotic for almost all planets and almost all initial conditions, with a Lyapunov time-scale of about 5–20 Myr. This seems to indicate that the addition of the inner planets adds more chaos to the system. Finally, we show that if we instead remove the outer planets and look at the isolated five-body system of the Sun + four terrestrial planets, then the terrestrial planets alone show *no* evidence of chaos at all, over a large range of initial conditions inside the observational error volume. We thus conclude that the uniformity of chaos in the outer planets comes not from the inner planets themselves, but from the interplay between the outer and inner ones. Interestingly, however, there exist rare and isolated initial conditions for which one individual outer planetary orbit may appear integrable over a 200-Myr time-scale, while all the other planets simultaneously appear chaotic.

Key words: celestial mechanics – ephemerides.

1 INTRODUCTION

Is the Solar system stable? Properly speaking, the answer is still unknown, and yet this question has led to very deep results which probably are more important than the answer to the original question.

Jürgen Moser

Astronomers have been interested in the phenomena of chaos in the Solar system for centuries, but reliable answers to the question of its stability have only been possible in the late 20th century due to the advent of numerical simulations fast enough accurately to integrate the Solar system for hundreds of millions of years. Direct numerical integration of the outer Solar system (henceforth SS for brevity) on the time interval of 100 Myr demonstrates that the orbit of Pluto is chaotic (Sussman & Wisdom 1988). However, the mass of Pluto is far too small for its chaos to spread into the orbits of the Jovian planets over the life of the SS. Laskar (1989) performed a 200-Myr integration of the entire SS except Pluto using an extended version of the perturbation methods developed by Lagrange and Laplace. He showed that the inner SS (Mercury, Venus, Earth and Mars) is chaotic with a Lyapunov time of about 5 Myr, but he saw no chaos in the orbits of the outer planets. The chaos in the inner SS was soon verified by full numerical integration of all the planets, but here chaos was also observed in the outer planets (Sussman & Wisdom 1992). This led to uncertainty about the existence of chaos in the outer SS that was resolved by demonstrating that both chaotic and apparently regular orbits exist within observational uncertainty (Hayes 2007, 2008).

During the past few decades there have been many studies of chaos in the SS, a survey of which is beyond the scope of this paper. The work in this paper stems from the recent observation that within the observational error of the positions of the Jovian planets, there

★E-mail: wayne@ics.uci.edu

exist some initial conditions that result in chaos in this system, and other initial conditions that lead to no observable chaos over durations ranging from 200 Myr to 5 Gyr (Hayes 2007, 2008). We study two questions arising from this observation. First, if we measure the Lyapunov time for each point in a given cross-section of initial condition space (all within observational error), what structures do we observe? And secondly, how does this structure change if we re-introduce the inner planets into the system, and also include other effects such as general relativity (GR), the J_2 moment of the Sun and a J_2 moment of the Earth–Moon system designed to mimic the effect of our Moon on the inner SS?

2 STRUCTURE OF CHAOS IN THE ISOLATED FIVE-BODY SYSTEM OF OUTER PLANETS

We integrate for 200 Myr the isolated five-body system consisting of the Sun, Jupiter, Saturn, Uranus and Neptune using only Newtonian gravity and treating all objects as point particles with constant mass. The effects of the inner planets are crudely taken into account by adding their masses and momenta to those of the Sun. It has been shown, albeit with a small number of samples, that this system contains some initial conditions within observational uncertainty that show chaos on a Lyapunov time-scale of a few Myr, while other initial conditions also within observational uncertainty show no observable chaos on time-scales ranging from 200 Myr to 5 Gyr (Hayes 2007, 2008). The goal of our first experiment is simply to explore more fully the structure of Lyapunov times that exist in this system, with initial conditions that are (mostly) within observational error of their true positions. We take the 'canonical' initial condition of DE405 (Standish 1998) as the centre of our exploration. We take two-dimensional slices through initial condition space representing the semimajor axes of pairs of planets. The size of the slices are 10 parts in 10^7 (five parts in each direction). The actual observational uncertainties of Jupiter, Saturn, Uranus and Neptune are about 1, 3, 5 and 7 parts in 10^7, respectively. We used the integration code *N*-body Integrator (NBI) for the outer SS integrations, with a time-step of 38 d and standard IEEE754 double-precision floating point. We verified that these integration parameters give results that agree with the far more carefully checked small-time-step integrations used in (Hayes 2007, 2008), while being the most efficient method among the integrators tested in that study. We found that a time-step up to 38 d resulted in essentially no observable change in Lyapunov structure, while a time-step of 40 d resulted in complete 'breakdown' of the integrations. This is in fact one of the previously observed *advantages* of NBI's Cowell–Störmer integrator: results remain reliable for time-steps up to a certain threshold, beyond which the results become obviously unreliable. This is in stark contrast to symplectic methods, in which the accuracy of the results degrade smoothly and significantly, but with no obvious failure mode (Hayes 2007, 2008). It is possible that this defect in symplectic methods may be corrected with a careful adjustment of the initial conditions, for example by using 'warmup' (Saha & Tremaine 1992) or high-order symplectic correctors (Wisdom 2006), but this direction needs further exploration.

Figs 1–7 show high-resolution (80 × 80 pixel) maps for Saturn–Jupiter and Neptune–Uranus pairs. We observe linear patterns similar to those observed by Guzzo (Guzzo 2005), which were caused by the overlap of three-body resonances. The structure observed here is likely caused by similar resonance overlap, either three-body or perhaps even four-body. Fig. 5, which shows the cross-section when perturbing the semimajor axes of Uranus and Neptune, shows little structure but instead looks like random noise, suggesting perhaps

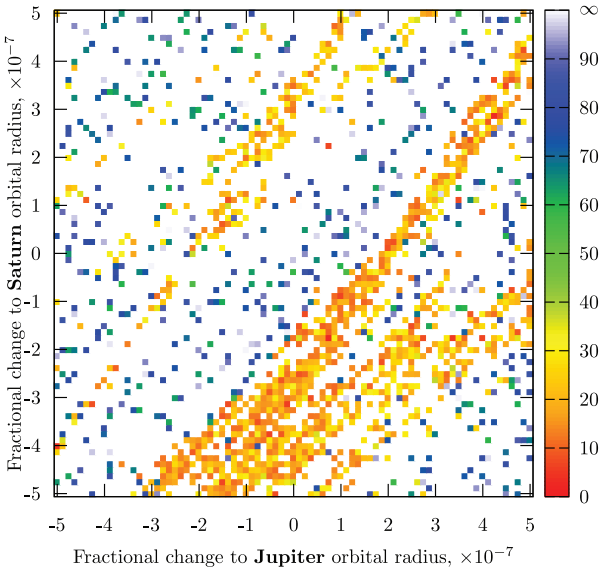

Figure 1. Lyapunov time map (in Myr) for perturbations in the semimajor axes of Jupiter and Saturn, outer SS integration only. The Lyapunov time is colour-coded, with red being zero Lyapunov time (i.e. an infinite Lyaponov exponent), and white being an infinite Lyapunov time (Lyapunov exponent of zero, indicating no chaos).

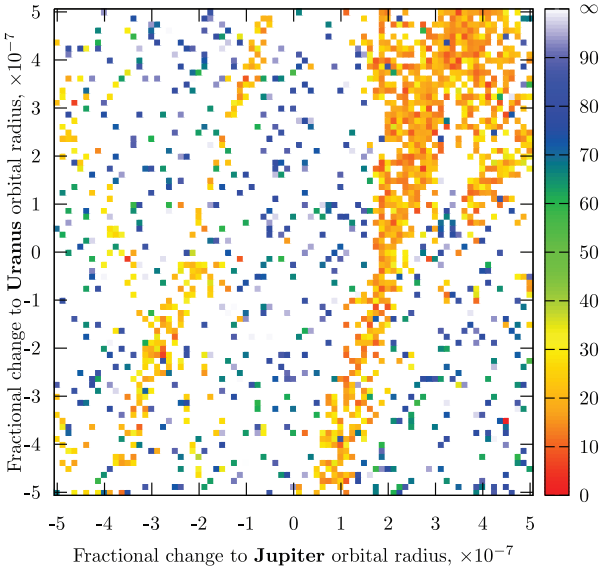

Figure 2. Lyapunov time map (in Myr) for perturbations in the semimajor axes of Jupiter and Uranus, outer SS integration only.

that significant changes in the structural stability at these scales require perturbation in at least one of Jupiter or Saturn. The Lyapunov time may vary from 5 Myr to infinity for initial conditions differing by 10^{-8} fractional part of semimajor axis of any Jovian planet. Fig. 7 shows a 'zoom' into a small region of Fig. 6 and illustrates that there exists tightly packed structure even at scales of one part in 10^9, consistent with fractal structure.

Although it is difficult to estimate the cumulative numerical error in our integrations, we find that energy error and the movement of the centre of mass of the system stay below about one part in 10^9 after 200 Myr. Furthermore, the observed structure below this level appears to be mostly random noise, indicating that Fig. 7 represents close to the limiting resolution of our 200-Myr integrations.

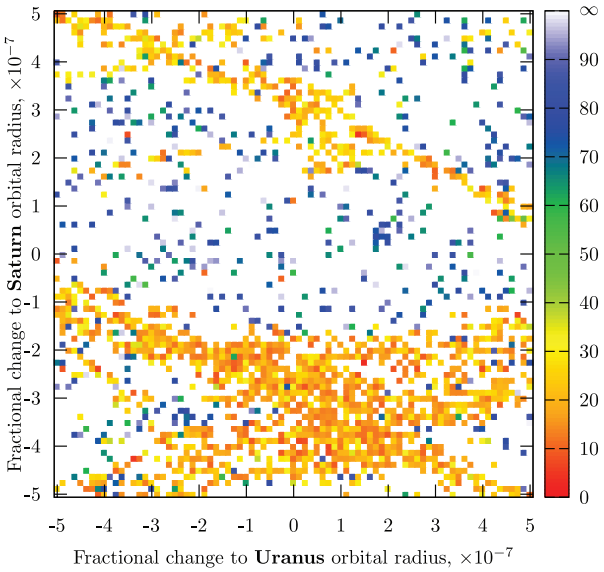

Figure 3. Lyapunov time map (in Myr) for perturbations in the semimajor axes of Saturn and Uranus, outer SS integration only.

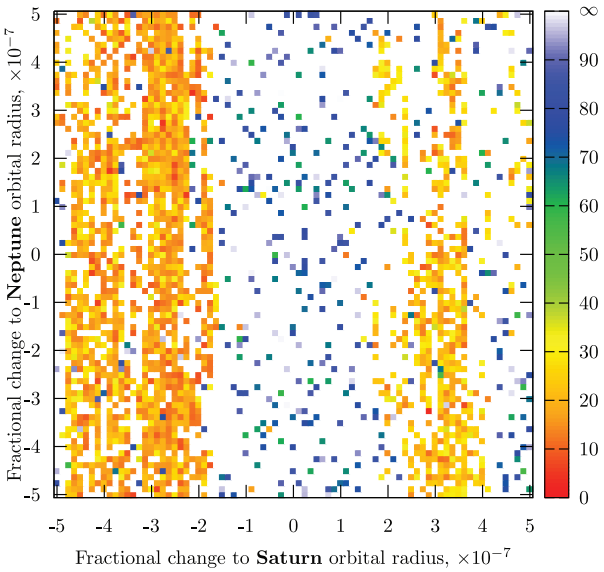

Figure 4. Lyapunov time map (in Myr) for perturbations in the semimajor axes of Saturn and Neptune, outer SS integration only.

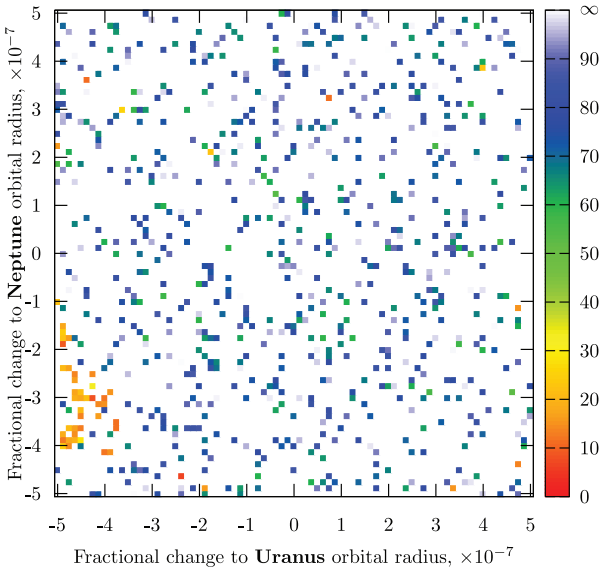

Figure 5. Lyapunov time map (in Myr) for perturbations in the semimajor axes of Uranus and Neptune, outer SS integration only.

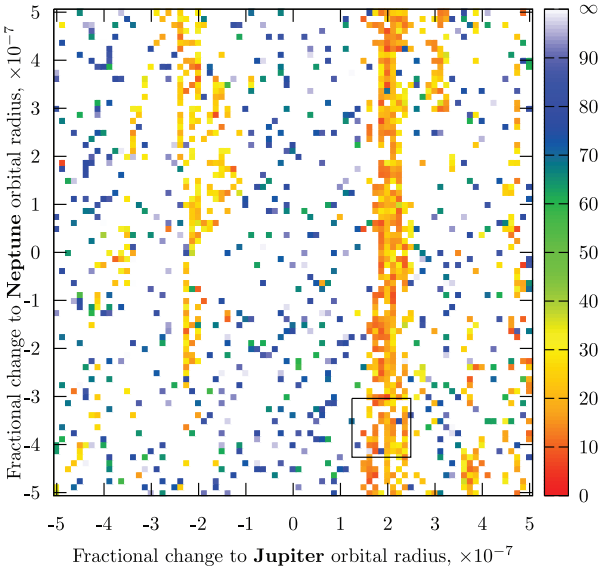

Figure 6. Lyapunov time map (in Myr) for perturbations in the semimajor axes of Jupiter and Neptune, outer SS integration only. The frame shows zoomed-in fragment presented in Fig. 7.

3 ADDING THE TERRESTRIAL PLANETS AND POST-NEWTONIAN CORRECTIONS

In order to test how the above structure changes in a significantly more realistic system, we perform a second set of 200-Myr simulations of the SS in which the terrestrial planets are included in the integration. In order to maximize the realism of the second system, we also add three more effects: (i) GR, (ii) the Sun's quadrupole moment and (iii) the Moon's effect on the inner SS is crudely taken into account by adding a quadrupole moment to the particle representing the Earth–Moon barycentre. All the details of the second system are taken directly from Varadi, Runnegar & Ghil (2003), as implemented in their (unpublished) extension of NBI, which they call Solar System Integrator with General Relativity (SSIGR). SSIGR uses the parametrized post-Newtonian formalism (PPN) to approximate the effects of GR and solar oblateness. Will (1993) provides a good overview of PPN and its applications. We neglect Pluto and all other bodies in the SS other than the Sun and largest eight planets. We ignore the mass-loss of the Sun because we have observed previously (Hayes 2008) that solar mass-loss has no observable effect on our results. (We briefly explore in Appendix A why this is likely to be the case.)

We tested the implementation of GR and the J_2 moment of the Sun by performing numerical integrations and measuring if the effects produced in our integrations agree with current theory and observations. We have measured the perihelion precession rate of Mercury's orbit in Newtonian gravity and in GR with all other parameters of the simulation being the same. The difference between these two precession rates gives us an effective precession

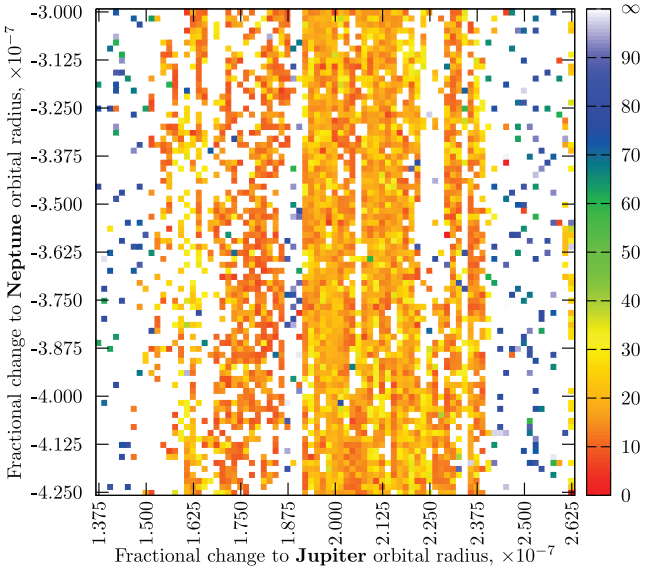

Figure 7. Zoom-in to Fig. 6. This map reveals fractal structure: vertical stable strip immediately adjacent to unstable areas separated by only one part in 10^9 – about 750 m in the semimajor axis of Jupiter or 6 km in the semimajor axis of Neptune.

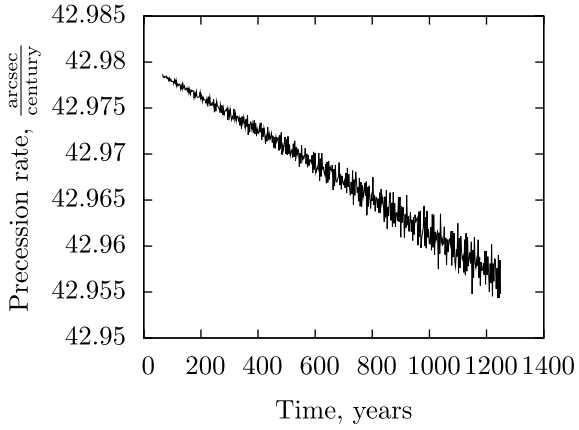

Figure 8. Testing our implementation of general relativity: excess perihelion precession rate of Mercury's orbit agrees with theoretical value of 42.98 arcsec century^{-1}.

rate, which is plotted in Fig. 8 on the time interval of 5×10^5 d. The effective precession rate induced by GR on this time interval is about 42.965 ± 0.015 arcsec century^{-1}, which is quite close to the theoretically predicted value of 42.98 ± 0.04 arcsec century^{-1} (Einstein 1916).

The value of the Sun's quadrupole moment J_2 is still quite uncertain, being about $(2.0 \pm 0.4) \times 10^{-7}$ (Pireaux & Rozelot 2003). Fig. 9 shows the dependence of extra precession rate on the J_2 value. Since it is a much smaller effect than that induced by GR we do not expect it to have a large effect on the system. In our simulations we have taken the value $J_2 = 2.18 \times 10^{-7}$ (Pijpers 1998).

The Moon is the most massive satellite in the SS relative to its parent planet. However, the Moon's orbital period is only about 27 d compared to Mercury's 88 d and it is too expensive to simulate the Moon as a separate body because it would require us to reduce the time-step of the integration substantially. We take the usual route of modelling the Earth–Moon pair as a single body, but we additionally

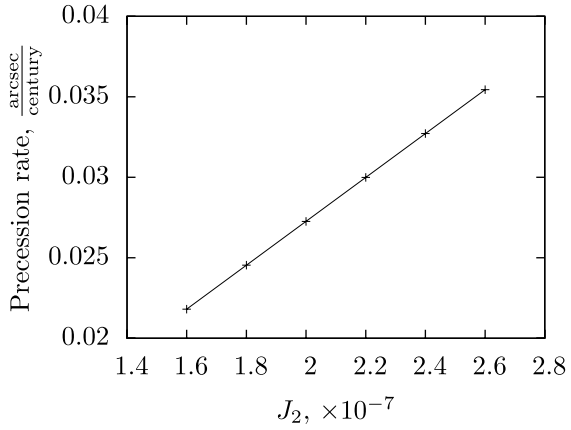

Figure 9. Testing our implementation of solar oblateness. The uncertainty in the excess perihelion precession rate of Mercury's orbit is about 0.15 arcsec century^{-1} (Pijpers 1998). This figure demonstrates that the precession rate is not strongly affected by the uncertainty in J_2 since the effect of J_2 is by several orders of magnitude smaller than other effects, such as GR.

give it a non-zero quadrupole moment. The Earth–Moon correction in SSIGR is implemented after (Quinn, Tremaine & Duncan 1991). Unfortunately we were not able to conduct the same test of the Earth–Moon correction as we did for GR and solar oblateness. One of the main reasons is that the Earth–Moon correction effect is much less significant than the former two effects. Quinn et al. (1991) performed some limited testing of the correction by comparing the integrations with and without the Earth–Moon correction. They came to the conclusion that the Earth–Moon correction factor (that we use) is accurate to within 1 per cent of the observations. Finally, Varadi et al. (2003) go through significant effort to match the Earth–Moon correction factor in SSIGR so that it gives results that match as closely as possible to integrations that include the Moon as a separate body.

4 THE INTERPLAY OF CHAOS BETWEEN THE INNER AND OUTER PLANETS

The uncertainty in the positions of Jupiter and Saturn is roughly 10^{-7} of their respective semimajor axes, while for Uranus and Neptune it is a bit larger (Standish 1998; Morrison & Evans 1998). Therefore, the uncertainty span for Jupiter and Saturn is about 16 pixels and for Uranus and Neptune it is about 40 pixels in Figs 1 and 5.

We have managed to obtain only low-resolution 9×9 pixel maps for the Saturn–Jupiter and Neptune–Uranus cross-sections shown in Figs 10 and 11. As can be seen, the entire region is uniformly chaotic, with Lyapunov times comparable to that measured for the inner SS by others. This is in stark contrast to the figures for the isolated outer SS, which can show large regions of initial condition space which admit no observable chaos over a 200-Myr time-scale. We conclude that the observed uniformity of chaos comes from an interplay between the inner SS and the outer SS.

If we look at the orbital divergence on a planet-by-planet basis rather than as an entire system, we find that there are rare, isolated initial conditions in which one planet's orbit shows a zero Lyapunov exponent while all the others in the same integration show a positive one. Fig. 12 illustrates an example. This is interesting, as it seems to say that although chaos can 'spread' through the entire system, it does not necessarily spread uniformly to all components of the system.

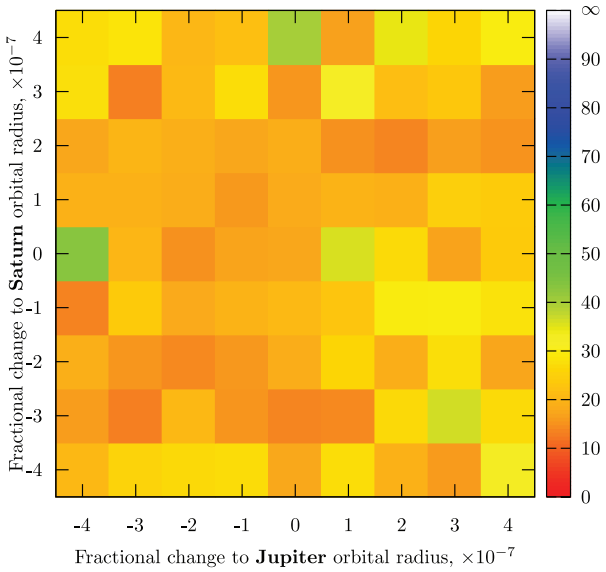

Figure 10. Lyapunov time map for perturbations in the semimajor axes of Saturn and Jupiter, entire SS integration.

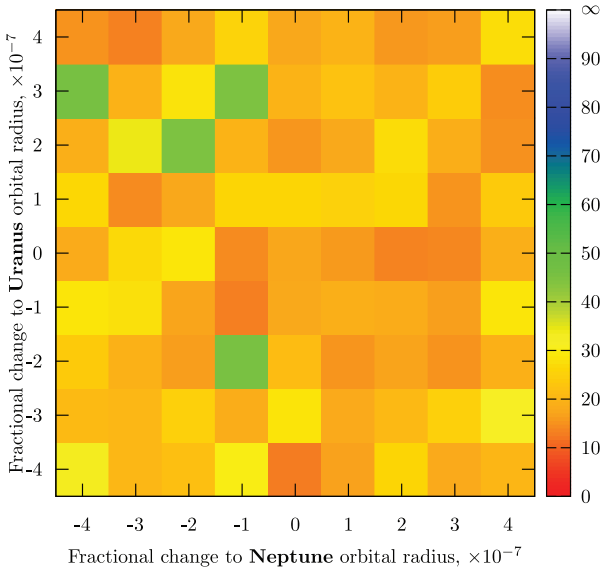

Figure 11. Lyapunov time map for perturbations in the semimajor axes of Uranus and Neptune, entire SS integration.

5 THE ISOLATED TERRESTRIAL PLANETS ADMIT NO CHAOS

We performed a suite of integrations of *just* the Sun + inner planets, without the presence of the Jovians. We used time-steps of 8, 4, 2 and 1 d; all time-steps agreed with each other. We found not a single initial condition that led to chaos on a 200-Myr time-scale. This is at least a little bit surprising given that integrations of the entire SS seem to show that the inner planets are chaotic (e.g. Laskar 1995, 1997, 1999; Varadi et al. 2003; Laskar & Gastineau 2009). Thus, the chaos in the inner SS must come from the interplay with the Jovians. Furthermore, there is no chaos 'in the inner SS' that can 'leak' to the outer SS, so again most of the chaos in the outer SS (but not all of it) comes from an interplay with the inner planets. This may not be too much of a surprise since, for example, Laskar

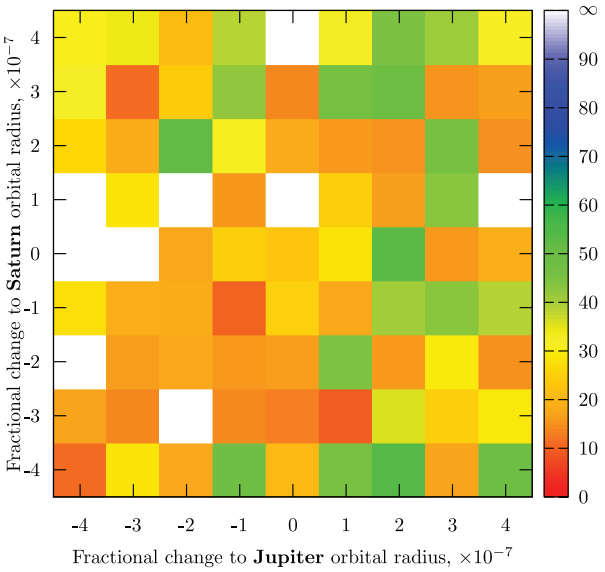

Figure 12. Divergence of Jupiter only; compare to Fig. 10. We see that although the system as a whole (in fact all three of the other outer planets) has a positive Lyapunov exponent, for some initial conditions Jupiter does not (white squares).

& Gastineau (2009) demonstrate that a large part of the chaos in the inner SS comes from a resonance between Mercury and Jupiter. Still, we found it surprising that the isolated inner SS shows *no* chaos at all.

6 NUMERICAL METHODS

6.1 Integration scheme

We used the code NBI for the outer SS integrations and its further development SSIGR for the entire SS integration. Both NBI and SSIGR use 14th-order Cowell–Störmer integrator with modifications by the UCLA research group led by William Newman (Newman et al. 1990), with a time-step of 38 d for the outer SS integrations, and a time-step of 0.65 d for the integrations that include the inner SS. We used standard IEEE754 double precision. We note in passing that Laskar (1995) uses a time-step of at most 40 d in order to integrate the outer SS and at most 0.5 d in order to integrate accurately the entire SS. However, his time-steps are tied to his particular integration scheme. To find the most efficient and reliable time-step for integrating the entire SS, we performed a number of test runs with different time-steps ranging from 0.30 to 0.80 d. The initial conditions were according to the DE405 ephemeris (Standish 1998). Fig. 13 shows the divergence of nearby trajectories for various time-steps from 0.40 to 0.80 d. Each line is significantly different from others, indicating a lack of convergence of results. We observe that the lines corresponding to the time-steps of 0.80 and 0.70 d exhibit exponential growth much earlier than the other lines. These three lines experience a sharp jump in the first 20 Myr, whereas the rest of the lines grow polynomially up to almost 60 Myr. We have determined that these jumps are primarily caused by the divergence of Mercury, to lesser extent by the divergence of Mars, the Earth–Moon barycentre and Venus, while the orbits of the outer planets are more stable. We conclude that a time-step of 0.65 d is an acceptable (but not ideal) value for the long-term integrations. Unfortunately we have not found any time-step that shows solid convergence to the

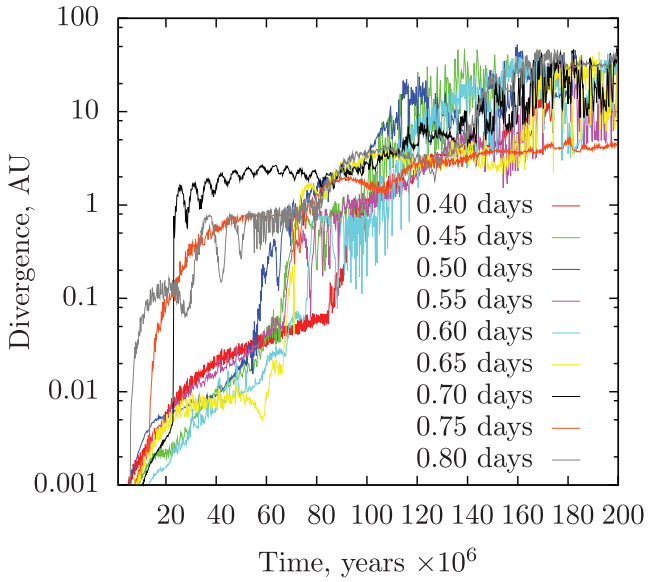

Figure 13. We found no convergence as the time-step goes down; however, integration with time-step 0.70 and larger show chaos due to numerical reasons.

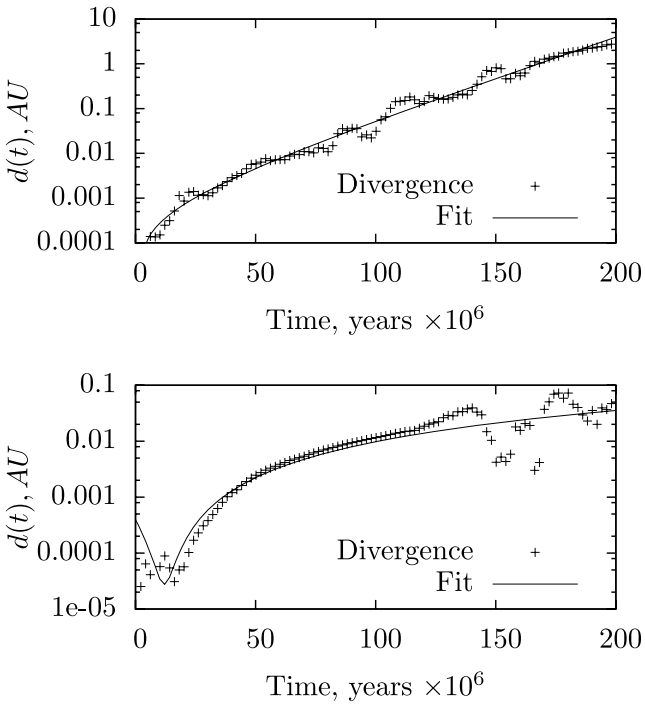

Figure 14. Estimating Lyapunov exponent by fitting $D(t) = ae^{\lambda t} + bt^{1.5} + c$ to the divergence data in logarithmic space.

true solution even over intervals as short as a few tens of millions of years, even though such convergence is easily achieved for the isolated outer SS (Hayes 2007, 2008). By 'solid convergence to the true solution' we mean a time-step below which all the sibling divergence diagrams have the same shape; this is different than saying that all the solutions have error smaller than some tolerance. For example, all solutions in Fig. 13 with time-steps of 0.65 d or less suggest that we can predict the positions of the inner planets to within about 0.05 au for at least 50 Myr; however, all the curves have different *shapes*, which indicates that we have not yet converged uniformly to the true solution. A similar lack of convergence has been reported by (Laskar & Gastineau 2009).

We believe that in order to see 'solid' convergence of the results for the inner SS requires a time-step much shorter than that which is currently feasible for a survey across initial conditions of the size we are performing; for example, a 38-d time-step for the outer SS corresponds to about 115 time-steps per orbit of Jupiter; a similar number of time-steps for Mercury's orbit would imply a time-step of 0.76 d. However, the time-scale over which an integration time-step dt is accurate scales as $e^{1/dt}$, when measured in the appropriate time-scale (Benettin & Giorgilli 1994; Reich 1999). Since Mercury orbits about 50 times for each orbit of Jupiter and $e^4 \approx 50$, the time-step may need to be another factor of 4 smaller, i.e. $0.76/4 = 0.19$ d. This would make our integrations take an unacceptably large amount of CPU time (and furthermore would increase the amount of round-off incurred during the integration). Thus, for now, we accept 0.65 d as our time-step for eight-planet integrations, and leave for the future the question of what time-step provides convergence of Lyapunov times for the inner SS.

Integration of the entire SS is far more expensive than integration of the outer SS alone for two reasons: (1) the time-step needs to be much smaller and (2) including the inner planets doubles the total number of planets, making each time-step about four times as expensive. As a result, integration of the entire SS is about 4700 times slower than integration of the outer SS alone. Each integration takes about 9 machine-days on a modern computer to complete. A typical computer in the cluster we used is either dual-processor, dual-core Opteron 2220 with 6 GB of RAM or dual-processor, quad-core Opteron 2356 with 12 GB of RAM.

6.2 Estimating the Lyapunov exponent

The Lyapunov exponent λ represents the exponentially fast separation rate between two trajectories separated by an infinitesimal amount. We estimate the Lyapunov exponent of a particular trajectory by performing a second integration starting with the position of Uranus perturbed by 10^{-14} au in the z direction; we then fit the distance $d(t)$ between the two trajectories to a curve of the form $D(t) = ae^{\lambda t} + bt^{1.5} + c$. The $t^{1.5}$ term models the numerical error that accumulates in a numerical trajectory whose numerical error is dominated by round-off, according to Brouwer's law (Brouwer 1937). We use the Levenberg–Marquardt algorithm as implemented in MATHEMATICA 6.0 to find the best fit of the coefficients of $D(t)$ to the divergence data. We fit $D(t)$ in logarithmic space, that is we find the best fit of the coefficients of $\log D(t)$ to the set of the divergence data pairs $(t, \log d(t))$, where $d(t)$ is the value of divergence at time t. Fig. 14 illustrates fitting process in chaotic (top) and non-chaotic (bottom) cases. Fig. 15 illustrates a fit of the slope of the curve measuring the divergence between siblings in the non-chaotic case, and demonstrates that our integrations satisfy Brouwer's law and thus have error which is dominated by unbiased round-off (which is the best one can hope for in a numerical integration).

ACKNOWLEDGMENTS

AVM acknowledges the support of the Department of Computer Science at UC Irvine, where parts of this work contributed to his MSc dissertation. The authors thank the Vermont Advanced Computing Center of the University of Vermont for granting enough cluster time to perform all our experiments and analyses. We thank

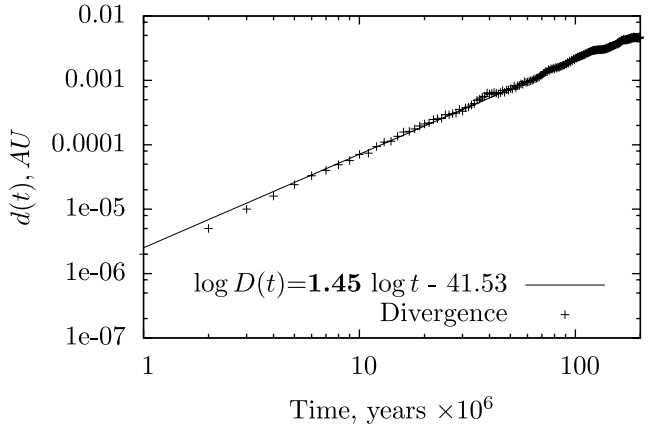

Figure 15. Our integrations satisfy Brouwer's law: the integration error grows polynomially with an exponent of about 1.45, demonstrating that our numerical error is dominated by unbiased round-off.

Scott Tremaine for the explanation in Appendix A about why solar mass-loss has negligible effect on our results.

REFERENCES

Benettin G., Giorgilli A., 1994, J. Statistical Phys., 74, 1117
Brouwer D., 1937, AJ, 46, 149
Einstein A., 1916, Ann. Phys., 49, 769
Guzzo M., 2005, Icarus, 174, 273
Hayes W. B., 2007, Nat. Phys., 3, 689
Hayes W. B., 2008, MNRAS, 386, 295
Laskar J., 1989, Nat, 338, 237
Laskar J., 1995, Gen. History Astron., 2B, 240
Laskar J., 1997, A&A, 317, L75
Laskar J., 1999, R. Soc. Lond. Philos. Trans. Ser. A, 357, 1735
Laskar J., Gastineau M., 2009, Nat, 459, 817
Morrison L. V., Evans D. W., 1998, A&AS, 132, 381
Newman W. I., Loh E., Kaula W. M., Doolen G. D., 1990, BAAS, 22, 950
Noerdlinger P. D., 2005, preprint (arXiv:0801.3807v1)
Pijpers F. P., 1998, MNRAS, 297, L76
Pireaux S., Rozelot J., 2003, Ap&SS, 284, 1159
Quinn T. R., Tremaine S., Duncan M., 1991, AJ, 101, 2287
Reich S., 1999, SIAM J. Numer. Analysis, 36, 1549
Saha P., Tremaine S., 1992, AJ, 104, 1633
Standish E. M., 1998, JPL Planetary & Lunar Ephemerides, DE405/LE405. Technical report, Jet Propulsion Laboratory
Sussman G. J., Wisdom J., 1988, Sci, 241, 433
Sussman G. J., Wisdom J., 1992, Sci, 257, 56
Varadi F., Runnegar B., Ghil M., 2003, ApJ, 592, 620
Will C. M., 1993, Theory and Experiment in Gravitational Physics, revised edn. Cambridge Univ. Press, Cambridge
Wisdom J., 2006, AJ, 131, 2294

APPENDIX A: WHY SOLAR MASS-LOSS DOES NOT MATTER?

The Sun loses about one part in 10^7 of its mass per Myr (Laskar 1999; Noerdlinger 2005). Thus, the orbits of the planets expand by about one part in 10^7 on a similar time-scale. Since the observational error volume is also about one part in 10^7, one might naïvely expect (as we did) that mass-loss will effect the observed structure of Lyapunov times within the observational error volume on a time-scale that is short compared to the Lyapunov time. However, we have observed (Hayes 2008) that solar mass-loss has absolutely no effect whatsoever on the observed structure of Lyapunov exponents.

The following explanation was offered by Scott Tremaine. We represent the orbital frequency of a planet by Ω_1 where $\Omega_1^2 = G(M + m_1)/a_1^3$, and m_1 and a_1 are the planetary mass and semimajor axis. Under slow evolution of the solar mass M, the adiabatic invariants of the orbit are conserved; these are the eccentricity and the angular momentum. Conservation of angular momentum means a_1 varies as $1/(M + m_1)$, so overall Ω_1^2 varies as $(M + m_1)^4$ under slow evolution of M. Write $M = M_0 + \mathrm{d}M$ where M_0 is the initial mass of the Sun and $\mathrm{d}M$ is its lost mass. Then

$$\Omega_1 = \Omega_{1,0}[1 + \mathrm{d}M/(M_0 + m_1)]^2,$$

where $\Omega_{1,0}$ is the initial value of Ω_1.

What matter for the fractal structure are the frequency ratios from different planets. For two planets 1 and 2 this ratio is

$$\Omega_1/\Omega_2 = (\Omega_{1,0}/\Omega_{2,0})f(t),$$

where

$$f(t) \approx [1 + \mathrm{d}M/(M_0 + m_1)]^2/[1 + \mathrm{d}M/(M_0 + m_2)]^2.$$

Since $\mathrm{d}M$ and m are both much less than M_0 but not so different from each other, we expand with this ordering to get

$$f(t) \approx 1 + 2(\mathrm{d}M/M_0)(m_2 - m_1)/M_0.$$

So over a 1-Gyr integration, solar mass-loss is about $\mathrm{d}M/M_0 \sim 10^{-4}$ and the planetary masses are of the order of $m/M_0 \sim 10^{-3}$; then $f(t) - 1$ is about 2×10^{-7}. So the maintenance of the resonances is not exact, but the evolution in frequency ratios is very small.

This paper has been typeset from a TEX/LATEX file prepared by the author.